

# Rapid Analysis of Heavy Metal Element Adsorption by SCG Based on LIBS Technology

Hairui Xie<sup>1</sup>, Libing You<sup>1,2,\*</sup>, Xiaodong Fang<sup>1,2</sup>, Leyi Li<sup>3</sup>, Haokai Ding<sup>3</sup>, Zhengqi Zhou<sup>3</sup>, Guanyang Zhang<sup>3</sup>, Dongjian Zhang<sup>3</sup>

<sup>1</sup>College of New Materials and New Energies, Shenzhen Technology University, Shenzhen, Guangdong, 518118, China

<sup>2</sup>Shenzhen Shengfang Technology Co., Ltd., Shenzhen, Guangdong, 518116, China

<sup>3</sup>Future Technology School, Shenzhen Technology University, Shenzhen, Guangdong, 518118, China

**Abstract.** Rapid evaluation and real-time detection of adsorption materials are particularly critical in the adsorption treatment of heavy metal wastewater. However, most elemental analysis methods have complex pretreatment procedures and are time-consuming, making real-time analysis difficult to achieve. A laser-induced breakdown spectroscopy device with a 248nm KrF excimer laser as the excitation source was used to study the rapid test of heavy metal content in wastewater absorbed by coffee grounds (SCG). This study prepared 16 sets of spent coffee grounds calibration samples and 8 sets of SCG adsorption samples by externally adding heavy metal elements. After optimizing the experimental system, the characteristic spectral lines of Cd II 226.510nm and Cu I 324.754nm were analyzed. Using Cu as the internal standard element, the Cd/Cu intensity ratios from the spectral tests of 16 calibration samples were fitted with the different Cd mass fractions in SCG to obtain a calibration model, with the polynomial fitting determination coefficient ( $R^2$ ) reaching 0.998. Eight adsorption samples were tested, and the calibration model was used to analyze the adsorption capacity of SCG for Cd solutions of different concentrations. The adsorption rate increased with the concentration of Cd solution, reaching a maximum of 18.96 mg/g. This work provides a reference for the rapid elemental analysis of adsorbent materials during the adsorption treatment of heavy metal wastewater.

## 1 Introduction

With the acceleration of urbanization and industrialization, the issue of heavy metal pollution has increasingly drawn attention. Heavy metals, due to their toxicity, persistence, ease of migration, bioaccumulation, and non-degradability, pose a significant threat to ecosystems and human health, severely damaging multiple organs in the human body [1-3].

How to remove heavy metals from wastewater is an important issue of concern in the fields of environment, materials, and engineering. Traditional methods for treating heavy metal wastewater include chemical precipitation, ion exchange, and electrochemical methods. However, these methods are costly, inefficient, energy-intensive, prone to material aging, and produce toxic by-products [4-5]. Adsorption methods, due to their safety, environmental friendliness, low maintenance costs, and simple technology, have unique advantages in treating heavy metal wastewater. The principle behind adsorption is the use of the high specific surface area and porous structure or special functional groups of adsorbent materials to adsorb heavy metal ions in water [6].

With the development concept of green environmental protection, more environmentally friendly and lower-cost biosorbents are currently being researched, such as tea waste, spent coffee grounds (SCG), bark, and fruit peels

[7-9]. Coffee is one of the largest agricultural products in the world, with approximately 170 countries being coffee-producing nations. In recent years, global coffee production is estimated to be over 160 billion 60-kilogram bags, resulting in millions of tons of coffee waste generated annually [10-11]. From the perspective of the circular economy, it is very suitable to produce adsorbents using waste generated from the coffee bean processing industry, and experimental studies have proven that SCG has a high adsorption capacity for heavy metals. Zhihua Deng et al. [12] significantly improved the adsorption capacity of SCG biochar through KOH modification, achieving maximum adsorption rates of 593 mg/g for Pb and 128 mg/g for Cd. Robyn Campbell et al. [13] prepared adsorbent samples from SCG under various pyrolysis conditions (temperature, treatment time, KOH mass) and evaluated their performance in removing  $\text{Cr}^{6+}$  from aqueous solutions, with the highest adsorption rate reaching 207 mg/g. Cybelle M. Futral et al. [14] investigated the performance of SCG as an adsorbent for treating actual soil washing wastewater, achieving maximum adsorption rates of 24.28 mg/g for Cu(II), 48.13 mg/g for Pb(II), and 5.25 mg/g for Zn(II) under conditions of 300 min and 328 K with 2.5 g of SCG.

In heavy metal adsorption treatment, it is necessary to monitor and evaluate the state of adsorption materials. Rapid measurement of heavy metal elements in adsorption

\* Corresponding author: [youlibing@sztu.edu.cn](mailto:youlibing@sztu.edu.cn)

materials is very important. In experiments, it enables the rapid evaluation of the optimal adsorption capacity of materials under different conditions. Industrially, it allows for real-time monitoring of whether the adsorption materials have reached saturation, helping to determine whether the adsorption materials need to be replaced in wastewater treatment to ensure the effectiveness of the treatment process. Currently, the main methods for heavy metal measurement include Inductively Coupled Plasma Mass Spectrometry (ICP-MS), Inductively Coupled Plasma Optical Emission Spectrometry (ICP-OES), and Atomic Absorption Spectrometry (AAS) [15-16]. The instrument cost of ICP-MS is high, maintenance is complex, and it has high requirements for sample pretreatment, necessitating the conversion of samples into transparent, homogeneous solutions for detection. Additionally, high-concentration samples may require dilution. ICP-OES has similar sample pretreatment requirements to ICP-MS, typically requiring samples to be digested into solutions, with sample pretreatment accounting for 90%-95% of the workload. AAS also requires samples to be processed into solution form, and

it usually can only detect the content of one element, making it unsuitable for simultaneous multi-element analysis.

Laser-Induced Breakdown Spectroscopy (LIBS) is an atomic or ionic emission spectroscopy technique that uses high-energy pulsed lasers to ablate materials, generating plasma. The characteristic spectral lines corresponding to elements produced by the plasma are collected and analyzed by a spectrometer, enabling qualitative and quantitative analysis of the elemental composition and content of solid, liquid, and gaseous substances. LIBS offers advantages such as rapid real-time analysis, no sample preparation required, non-destructive analysis, and multi-element measurement capabilities [17-18].

This study, based on LIBS technology, determined the calibration model for SCG with different cadmium contents after optimizing experimental parameters. Based on this model, the adsorption capacity of SCG for heavy metal element cadmium was analyzed, providing a basis for rapid elemental detection and analysis methods in the field of heavy metal adsorption treatment.

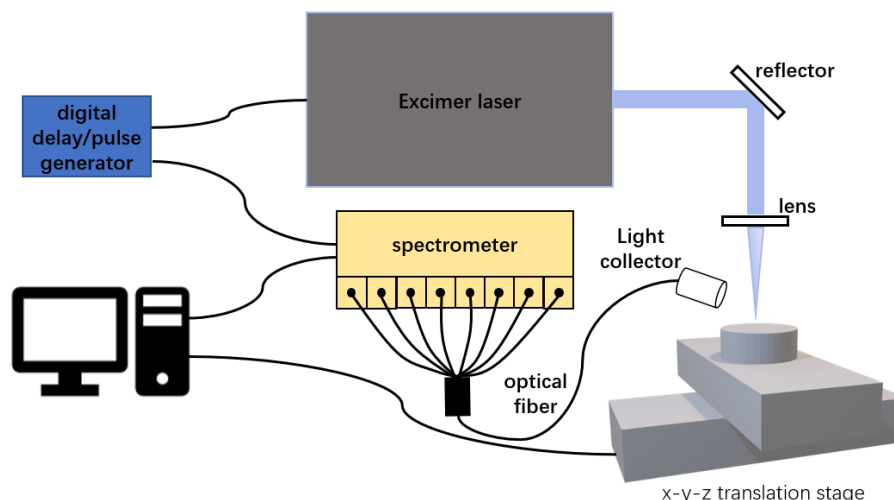


**Fig 1.** Schematic diagram of LIBS.

## 2 LIBS experimental system and sample preparation

### 2.1 LIBS experimental system

The excimer LIBS system constructed in the experiment is shown in Figure 1. The LIBS experimental system consists of a laser, optical system, fiber optic spectrometer, digital delay generator, computer, translation stage, and other components.

The DG645 digital delay generator offers multi-channel outputs with low jitter, high precision, and high trigger frequency. The delay resolution for all channels is 5ps, and the jitter between each channel is less than 25ps. The signals generated by the DG645 synchronize the control of lasers and spectrometers with different delay triggers.

The laser source employs an excimer laser PM248 (Shenzhen Shengfang Technology Co., Ltd), operating at a wavelength of 248nm, with a repetition rate of 1-20Hz,

pulse width of 30ns, and a maximum single pulse energy of approximately 650mJ. It supports external triggering with TTL level and allows adjustment of the discharge voltage to change the laser output energy. Excimer lasers offer advantages such as short wavelength and high photon energy, which effectively reduce thermal effects, shielding effects, and fractionation effects when applied in LIBS detection.

After the beam passes through multiple mirrors and is intercepted by a square aperture to capture an 8mm\*15mm laser spot, a UV focusing lens with a focal length of 100mm converges the spot into an image. The imaging spot is approximately 500um\*1200um, with a laser energy density of 8J/cm<sup>2</sup>-12J/cm<sup>2</sup>. The laser interacts with the sample, exciting the plasma. The plasma signal is coupled into an optical fiber through a collimating lens and transmitted to an eight-channel fiber optic spectrometer AVS-RACKMOUNT-USB2 (Beijing Avantes Technology Co., Ltd) for signal acquisition. The spectrometer, with a measurement range of 200nm-

1070nm and a minimum resolution of 0.06nm, was operated at its shortest integration time of 1.05ms for the work. To prevent the laser from collecting multiple data points from the same location, the sample was placed on

a translation stage 7SC3XX (Beijing Saifan Optoelectronic Instruments Co., Ltd), and data was collected only once at each position.

**Table 1.** Mass fraction of Cd in SCG.

No.	SCG /g	weight of the added Cd /mg	weight of the added Cu /mg	mass fraction of Cd(mg/g)
1	2	0.1	20	0.05
2	2	0.3	20	0.15
3	2	0.5	20	0.25
4	2	0.7	20	0.35
5	2	1	20	0.50
6	2	3	20	1.50
7	2	5	20	2.49
8	2	7	20	3.49
9	2	10	20	4.98
10	2	20	20	9.9
11	2	30	20	14.78
12	2	40	20	19.61
13	2	50	20	24.39
14	2	60	20	29.13
15	2	80	20	38.46
16	2	100	20	47.62

**Table 2.** SCG adsorption of different concentrations of cadmium solutions.

No.	SCG /g	weight of the added Cu /mg	mass fraction of Cd solution(g/L)
1	2	20	0.16
2	2	20	0.33
3	2	20	0.5
4	2	20	0.66
5	2	20	0.83
6	2	20	1
7	2	20	1.33
8	2	20	1.66

## 2.2 Sample preparation

The SCG used in the experiment was collected from a coffee shop in Shenzhen. The SCG was dried, and 16 equal portions of the SCG, each weighing 2g, were weighed using an electronic balance. A standard solution with a Cd concentration of 10mg/ml was prepared using cadmium nitrate tetrahydrate (Shanghai Macklin Biochemical Technology Co., Ltd.,  $\text{CdN}_2\text{O}_6 \cdot 4\text{H}_2\text{O}$ , 99.99%). A standard solution with a Cu concentration of 10mg/ml was prepared using copper nitrate (Shanghai Macklin Biochemical Technology Co., Ltd.,  $\text{Cu}(\text{NO}_3)_2$ , 98%).

Different amounts of Cd standard solution were added to SCG as calibration samples. The same amount of Cu standard solution was added to each SCG sample as an internal standard element. Pure water was added to ensure uniform mixing, and after drying, 300mg of the sample was taken, pressed into a disc with a diameter of 10mm and a thickness of 3.5mm using a pellet press at 10MPa for 10 minutes. The samples were numbered according to the mass fraction of Cd element, as shown in Table 1.

Prepare solutions with different concentrations of Cd. Use an electronic balance to weigh eight equal portions of SCG, each 2g, and place them separately into different concentrations of Cd solutions for stirring and adsorption.

After 5 minutes of adsorption, separate the solid and liquid phases, and take the adsorbed SCG. Add Cu standard solution to each sample to configure SCG samples with the same mass fraction of Cu as shown in Table 1. After drying, take 300mg of the sample and use a pellet press to maintain it at 10MPa for 10 minutes, compressing the SCG sample into a disc with a diameter of 10mm and a thickness of 3.5mm. Number the samples according to the different concentrations of Cd solutions, as shown in Table 2.

## 3 Analysis

### 3.1 SCG's spectral testing

The LIBS measurements were conducted on the SCG pellet samples from Table 1 and Table 2, respectively, recording spectral data in the wavelength range of 200-1070 nm, as shown in Figure 2 Based on relevant literature and the atomic spectral database of the National Institute of Standards and Technology (NIST), the original elements Ca, Mg, Na, K, and the added elements Cd and Cu were identified in the SCG.

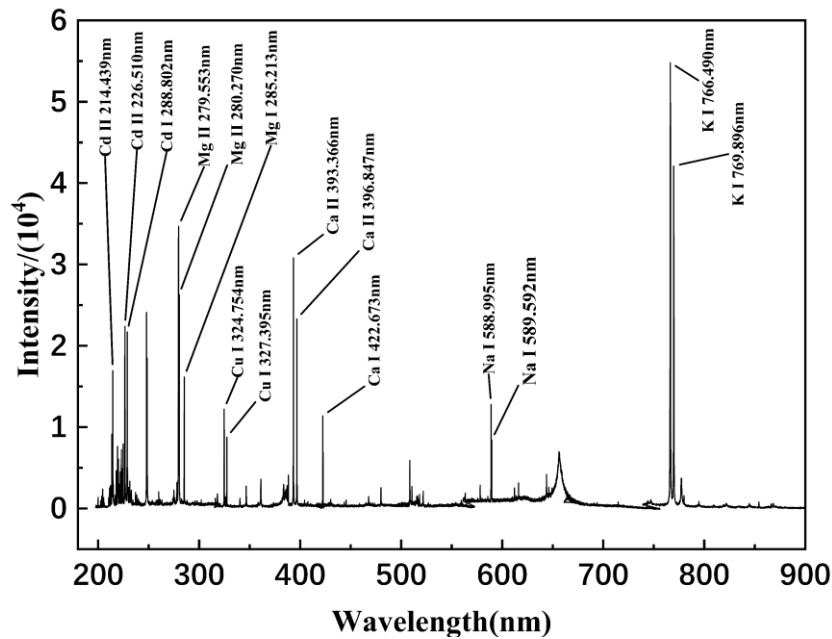


**Fig 2.** Spectrogram of SCG.

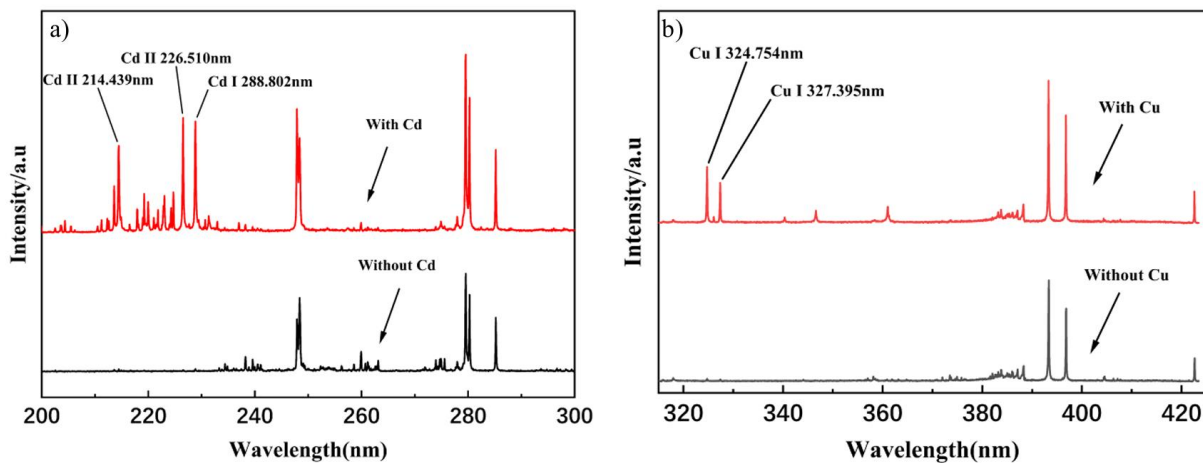


**Fig 3.** spectrogram of SCG containing different elements(a)with Cd and without Cd;(b) with Cu and without Cu.

By analyzing and comparing the spectra of blank samples and SCG containing Cd and Cu, two characteristic peaks with less interference and no significant self-absorption effect were selected, namely Cd II 226.510nm and Cu I 324.754nm. Figures 3(a) and 3(b) show the spectra at the characteristic peaks of Cd and Cu, respectively. Comparing the samples containing Cd and Cu with the blank samples, it can be seen that no Cd and Cu elements were detected in the blank samples.

### 3.2 Effect of Delay Time on Spectral Signals

As a transient pulsed plasma source, the radiation intensity of laser-induced plasma varies with time, so the delay time of measurement has a significant impact on the spectral results. During the generation and dissipation of the plasma, continuous background radiation, ionic line radiation, and atomic spectral line radiation are produced, each with different generation times and decay rates.

In the early stages, due to the strong background radiation signal, even with a relatively high spectral signal intensity, background noise still significantly affects the collection of plasma atomic spectra, resulting in a low Signal-to-Background Ratio (SBR). Over time, both the spectral signal and background noise signals gradually decay, but the background noise decays faster than the atomic spectral line radiation. As the intensity of the spectral signal weakens, the SBR correspondingly increases. Based on this, LIBS measurements typically find the optimal delay node for collecting spectra at different time resolutions to ensure both high spectral intensity and SBR when collecting characteristic spectra.

Figure 4 illustrates the effect of different spectral measurement delay times (0-0.7 $\mu$ s) on the characteristic spectral line signals of Cd and Cu in SCG, using Sample 1 from Table 1. Figure 4(a) shows that the Cd spectral signal reaches its highest intensity at a delay of 0.1 $\mu$ s, but due to significant background noise, the Signal-to-Background Ratio (SBR) is low. As the delay increases, the signal weakens and the SBR gradually improves. Figure 4(b)

demonstrates a similar trend for the Cu spectral signal, but since the concentration of Cu is higher compared to Cd, the measured spectral intensity is greater, and the impact of background noise is less significant, allowing the SBR to remain consistently higher than that of the Cd spectral data. Therefore, a test delay time of 0.5  $\mu$ s is selected.

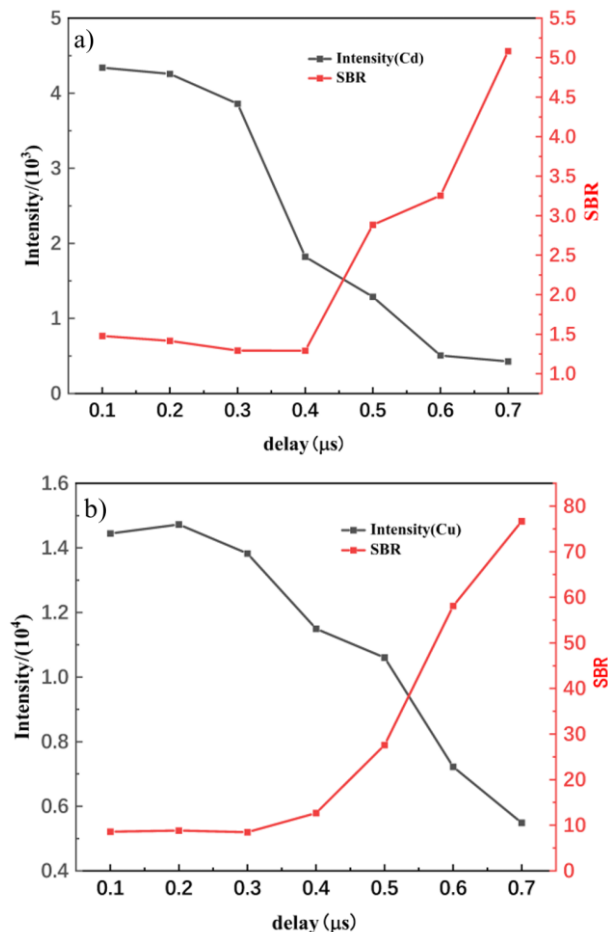


**Fig 4.** Effects of delay time on spectral signals  
 (a) Cd II 226.510nm; (b) Cu I 324.754nm.

### 3.3 Effect of Laser Energy on Spectral Signals

As a plasma excitation source, different laser energy densities lead to changes in spectral intensity. Generally, as energy density increases, both spectral intensity and background noise intensity rise, and the signal becomes more unstable. For different test samples and different characteristic spectral lines, it is necessary to select an appropriate laser energy density for experimentation.

In this work, the size of the laser-material interaction area was kept constant, and an energy range of 40-75 mJ was set, with energy adjustments tested every 5 mJ. The spectrometer delay was set to 0.5  $\mu$ s, and the experimental sample was sample 4 in Table 2. Figures 5(a) and (b) show the changes in the Cd and Cu characteristic spectral lines under different energies, respectively. It can be seen that the spectral intensities of both increase with the increase in laser energy. However, the SBR development patterns of Cd and Cu are quite different. The reason is that as the laser energy increases, the enhancement of the Cd

characteristic peak is much higher than that of the background noise and the Cu characteristic peak, so its SBR continues to increase with the energy; while the enhancement of the Cu characteristic peak with increasing laser energy is relatively small, making the background noise a more significant factor affecting the SBR.

With increased energy, the sample ablation amount also increases, and the signal becomes more unstable. Considering all factors, a laser energy of 60mJ is selected.

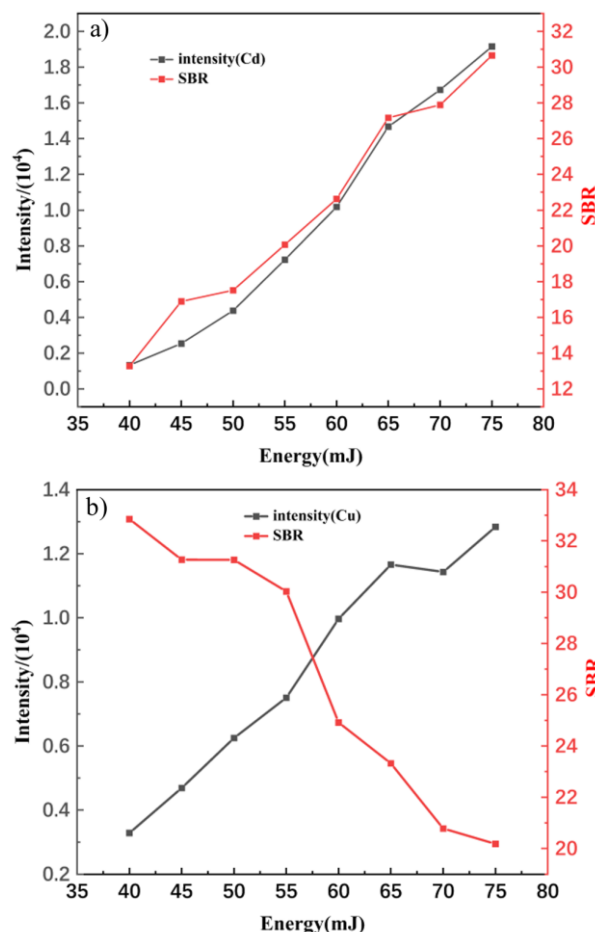


**Fig 5.** Effects of laser energy on spectral signals  
 (a) Cd II 226.510nm; (b) Cu I 324.754nm.

### 3.4 Quantitative Analysis of Cd in SCG

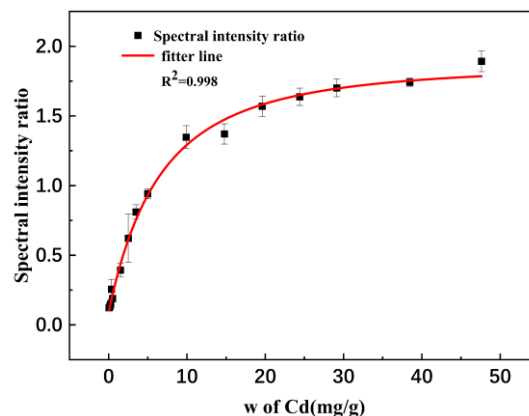


**Fig 6.** Calibration curves with internal standard method  
 (Intensity ratio of Cd II 226.510 nm and Cu I 324.754nm).



Due to the effects of matrix effects, surface roughness, experimental equipment jitter, and environmental fluctuations on the experimental samples, even under the same conditions of manually controlling laser energy and acquisition delay, the excitation radiation state of the plasma is difficult to maintain good stability. If the external standard method is used, and calibration analysis is directly performed using the peak values of the original spectral features, the stability is relatively low. Compared to the external standard method, the internal standard method is less affected by fluctuations in experimental conditions and can effectively overcome the influence of laser energy fluctuations and changes in sample surface.

Using Cu as an internal standard to determine Cd content in SCG samples with varying Cd concentrations, the spectral lines Cd II 226.510 nm and Cu I 324.754 nm were selected for calibration analysis. Both characteristic lines exhibit good spectral intensity, minimal interference, and good stability. Figure 6 shows the ratio of Cd II 226.510 nm to Cu I 324.754 nm for LIBS results at different Cd concentrations, with the samples measured as listed in Table 1. The standard deviation of the measurement data is used as the error bar. At relatively low concentrations, the calibration results are relatively linear. As the concentration increases, the calibration curve for Cd gradually bends due to self-absorption effects. A polynomial fit was used, with a coefficient of determination  $R^2$  of 0.998.

### 3.5 LIBS detection of SCG' adsorption capacity for water solutions with varying Cd concentrations

The LIBS test was performed on SCG samples adsorbed with different concentrations of Cd solutions as shown in Table 2. The Cd/Cu intensity ratio is presented in Figure 7. Using the calibration model measured in Figure 6 as a reference, the Cd adsorption capacity of SCG in Table 2 samples for different concentrations of Cd solutions was determined, with the results shown in Figure 7. It can be seen that SCG effectively adsorb Cd. As the concentration of Cd solution increases, the adsorption capacity of Cd also gradually increases. In the solution concentration settings of this study, the maximum adsorption rate of Cd by SCG was 18.96 mg/g.

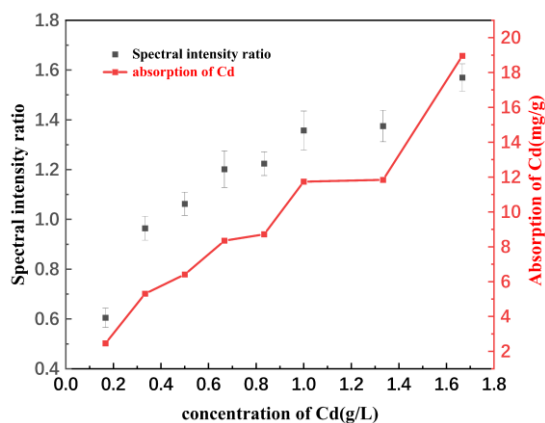


**Fig 7.** Spectral intensity ratio and adsorption capacity of SCG adsorbing solution with different Cd concentration.

## 4 Conclusion

When detecting and analyzing SCG samples containing heavy metal Cd using LIBS, the spectral intensity signal is not stable enough due to the influence of laser energy and background signals. To improve the signal-to-background ratio of the experiment, the experimental conditions were first optimized, and then appropriate characteristic spectral lines were selected for detection and analysis. The internal standard method was used to quantitatively analyze the differences in Cd content in SCG, and the results of the internal standard calibration model showed a high degree of fitting. Based on the quantitative analysis calibration model results, the adsorption capacity of SCG for Cd was detected in Cd solutions with different concentrations. The results showed that SCG can effectively adsorb Cd, and as the concentration of Cd solution increases, the adsorption capacity of SCG also increases accordingly. In the solution concentration settings of this study, the maximum adsorption rate of 2g of SCG was 18.96mg/g.

The research results have certain reference value for the evaluation of adsorption materials and real-time monitoring of element rapid detection analysis in the process of heavy metal wastewater adsorption treatment.

## Acknowledgments

This work is supported by Key-Area Research and Development Program of Guangdong Province (2023B0909010003), National Natural Science Foundation of China (62175167), Guangdong Provincial Science and Technology Program (2021QN02Z552), Guangdong province key construction discipline scientific research ability promotion project (2021ZDJS112) and Shenzhen Science and Technology Program (JCYJ20210324120207021, JSGG20220831094202005 and KQTD20170331115422184).

## References

1. Mwandira W, Nakashima K, Togo Y, et al. Cellulose-metallothionein biosorbent for removal of Pb (II) and Zn (II) from polluted water[J]. Chemosphere, 2020, 246: 125733.
2. Zhou L, Li N, Jin X, et al. A new nFe@ ZIF-8 for the removal of Pb (II) from wastewater by selective adsorption and reduction[J]. Journal of colloid and interface science, 2020, 565: 167-176.
3. Ahmed M J K, Ahmaruzzaman M. A review on potential usage of industrial waste materials for binding heavy metal ions from aqueous solutions. J Water Process Eng 10: 39–47[J]. 2016.
4. Jiang Lai, Wu Bang, Guo Xin, et al. Application of biochar in the remediation of heavy metal-contaminated lake sediments [J]. Water Treatment Technology, 2022, 48(04): 24-29+41. DOI: 10.16796/j.cnki.1000-3770.2022.04.005.
5. Honarmandrad Z, Javid N, Malakootian M. Efficiency of ozonation process with calcium peroxide in removing heavy metals (Pb, Cu, Zn, Ni,

- Cd) from aqueous solutions[J]. *SN Applied Sciences*, 2020, 2(4): 703.
6. Feng Jiangtao, Wang Zhenyu, Yan Xuanye, et al. Research progress on influencing factors of adsorption removal of heavy metal ions in water [J]. *Journal of Xi'an Jiaotong University*, 2022, 56(02): 1-16.
  7. Yilmaz O, Tugrul N. Zinc adsorption from aqueous solution using lemon, orange, watermelon, melon, pineapple, and banana rinds[J]. *Water Practice & Technology*, 2022, 17(1): 318-328.
  8. Minamisawa M, Minamisawa H, Yoshida S, et al. Adsorption behavior of heavy metals on biomaterials[J]. *Journal of agricultural and food chemistry*, 2004, 52(18): 5606-5611.
  9. Sharifi M J, Nouralishahi A, Hallajisani A. Fe<sub>3</sub>O<sub>4</sub>-chitosan nanocomposite as a magnetic biosorbent for removal of nickel and cobalt heavy metals from polluted water[J]. *International Journal of Biological Macromolecules*, 2023, 248: 125984.
  10. Lee Y G, Cho E J, Maskey S, et al. Value-added products from coffee waste: a review[J]. *Molecules*, 2023, 28(8): 3562.
  11. Freitas V V, Borges L L R, Vidigal M C T R, et al. Coffee: A comprehensive overview of origin, market, and the quality process[J]. *Trends in Food Science & Technology*, 2024: 104411.
  12. Deng Z, Ma P, Xiang P. The mechanism of Pb (II) and Cd (II) removal by coffee grounds biochar: Role of KOH modification[J]. 2023.
  13. Campbell R, Xiao B, Mangwandi C. Production of activated carbon from spent coffee grounds (SCG) for removal of hexavalent chromium from synthetic wastewater solutions[J]. *Journal of Environmental Management*, 2024, 366: 121682.
  14. Futralan C M, Kim J, Yee J J. Adsorptive treatment via simultaneous removal of copper, lead and zinc from soil washing wastewater using spent coffee grounds[J]. *Water Science and Technology*, 2019, 79(6): 1029-1041.
  15. Niu Yukun. Analysis of Heavy Metal Detection Technology in Water Bodies and the Latest Research Progress [J]. *Shandong Chemical Industry*, 2024, 53(11): 108-110. DOI: 10.19319/j.cnki.issn.1008-021x.2024.11.014.
  16. You Zhengkai. Research on LIBS Detection Method for Heavy Metals Chromium, Cadmium, and Lead in Water Bodies [D]. *Zhejiang University*, 2023. DOI: 10.27461/d.cnki.gzjdx.2023.002724.
  17. Zhao Nanjing, Gu Yanhong, Meng Deshuo, et al. Research Progress of Laser-Induced Breakdown Spectroscopy Technology [J]. *Journal of Atmospheric and Environmental Optics*, 2016, 11(05): 367-382.
  18. Gardette V, Motto-Ros V, Alvarez-Llomas C, et al. Laser-induced breakdown spectroscopy imaging for material and biomedical applications: recent advances and future perspectives[J]. *Analytical Chemistry*, 2023, 95(1): 49-69.